JACS
JOURNAL OF THE AMERICAN CHEMICAL SOCIETY
Article
pubs.acs.org/JACS

A Molten Salt Lithium–Oxygen Battery

Vincent Giordani,[*,†] Dylan Tozier,[‡] Hongjin Tan,[†] Colin M. Burke,[∥,⊥] Betar M. Gallant,[§] Jasim Uddin,[†] Julia R. Greer,[‡] Bryan D. McCloskey,[∥,⊥] Gregory V. Chase,[†] and Dan Addison[*,†]

[†]Liox Power, Inc., 129 N. Hill Ave., Pasadena, California 91106, United States
[‡]Division of Engineering and Applied Science, California Institute of Technology, Pasadena, California 91125, United States
[§]Division of Chemistry and Chemical Engineering, California Institute of Technology, Pasadena, California 91125, United States
[∥]Department of Chemical and Biomolecular Engineering, University of California, Berkeley, California 94720, United States
[⊥]Energy Storage and Distributed Resources Division, Lawrence Berkeley National Laboratory, Berkeley, California 94720, United States

Supporting Information

ABSTRACT: Despite the promise of extremely high theoretical capacity ($2Li + O_2 \leftrightarrow Li_2O_2$, 1675 mAh per gram of oxygen), many challenges currently impede development of Li/O_2 battery technology. Finding suitable electrode and electrolyte materials remains the most elusive challenge to date. A radical new approach is to replace volatile, unstable and air-intolerant organic electrolytes common to prior research in the field with alkali metal nitrate molten salt electrolytes and operate the battery above the liquidus temperature (>80 °C). Here we demonstrate an intermediate temperature Li/O_2 battery using a lithium anode, a molten nitrate-based electrolyte (e.g., $LiNO_3$–KNO_3 eutectic) and a porous carbon O_2 cathode with high energy efficiency (~95%) and improved rate capability because the discharge product, lithium peroxide, is stable and moderately soluble in the molten salt electrolyte. The results, supported by essential state-of-the-art electrochemical and analytical techniques such as in situ pressure and gas analyses, scanning electron microscopy, rotating disk electrode voltammetry, demonstrate that Li_2O_2 electrochemically forms and decomposes upon cycling with discharge/charge overpotentials as low as 50 mV. We show that the cycle life of such batteries is limited only by carbon reactivity and by the uncontrolled precipitation of Li_2O_2, which eventually becomes electrically disconnected from the O_2 electrode.

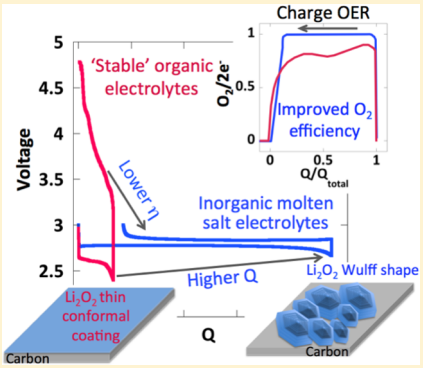

1. INTRODUCTION

Lithium-ion batteries (LIBs) are currently the state-of-the-art technology for high-energy electrochemical storage. LIBs employ intercalation materials, such as graphitic carbon anodes and transition metal oxide cathodes that host the lithium ions as the battery charges and discharges. The capacity of a Li-ion battery is dictated by the amount of Li^+ that can be reversibly extracted from/inserted in the crystal structure of the intercalation materials. For example, in the positive electrode (cathode), which typically limits the overall battery capacity, slightly less than one Li^+ ion can be stored per transition metal atom, which limits the active material specific capacity to 140–200 mAh per gram. Although LIBs currently provide the best properties for a high-energy, high-power, and long-life battery, many emerging markets, including electric vehicles, demand battery energy densities that may not be achieved by LIBs.

Therefore, new chemistries, such as lithium–sulfur, magnesium–ion, and lithium–air (oxygen), are being explored as high-energy alternatives to state-of-the-art LIBs. In particular, lithium–air (Li/O_2) batteries have received significant interest in the past decade, because, in principle, coupling lithium metal to oxygen could lead to the most energy dense electrochemical system[1−4] (Li_2O_2, the desired discharge product, provides a theoretical capacity of 1675 mAh/g). However, finding sufficiently stable electrolytes in the presence of the active Li/O_2 cathode electrochemistry has been the most elusive challenge to date.[5−7] Oxygen reduction in Li^+-bearing nonaqueous organic electrolytes has been widely studied, and regardless of the electrolyte composition, parasitic reactions occur between the reduced oxygen species that form during battery discharge, such as superoxide anion O_2^-, lithium superoxide LiO_2 and lithium peroxide Li_2O_2, and the electrolyte constituents (solvent and salt).[8−10] The resultant parasitic reaction products are typically insoluble and electronically insulative, and therefore gradually passivate the cathode during battery cycling. Although passivation of the cathode by parasitic products may be alleviated by oxidative removal during battery charge, the high overpotentials necessary to oxidize them lead to low round-trip energy efficiencies (typically around 65%, compared to >98% in state-of-the-art LIBs). Obviously, continuous formation and oxidation of side products associated

Received: November 9, 2015
Published: February 12, 2016

DOI: 10.1021/jacs.5b11744
J. Am. Chem. Soc. 2016, 138, 2656–2663

with parasitic side reactions also limit battery cycle life. As a result, electrolyte instability in the Li/O_2 battery presents the single largest scientific hurdle in their development as a practical energy storage device.

An additional challenge related to Li/O_2 batteries is the insulating and insoluble nature of lithium peroxide, the discharge product of the battery. As Li_2O_2 forms during discharge, it passivates the cathode surface, limiting discharge capacity to a small fraction of the large theoretical capacity provided by the Li/O_2 electrochemistry. Furthermore, the mechanism of Li_2O_2 formation in certain electrolytes leads to the formation of large Li_2O_2 agglomerates in the cathode, resulting in high polarization during battery charge associated with charge transport through the agglomerates. To overcome this issue, researchers have investigated soluble catalysts, known as redox mediators, to facilitate lithium peroxide oxidation during battery charge.[11,12] However, chemical instability of this class of materials during battery operation remains an unsolved problem.

Our approach is to replace unstable aqueous or organic-based electrolytes common in prior Li/O_2 battery research with an organic-free molten alkali metal nitrate electrolyte and operate the battery above the eutectic melting point, typically between 80 and 200 °C.[13] Research on molten nitrate electrolytes for lithium batteries and thermal batteries traces back to the late 1970s[14,15] when it was observed that the reaction between metallic lithium and the nitrate anion generated a SEI composed of lithium oxide (Li_2O) that was sufficiently stable for primary cells and rechargeable cells with limited cycle life. However, reports on O_2 electrode behavior in these electrolyte mixtures are somewhat lacking. Zambonin et al. reported that equilibria between superoxide, peroxide and oxide forms of reduced oxygen could coexist in the molten salt electrolyte with high reversibility at a Pt rotating disk electrode.[16,17] Stability toward Li, low melting point relative to other inorganic salts, high thermal stability above 500 °C, nonvolatility, high ionic conductivity and acceptable electrochemical stability window (typically between 2.2 and 3.8 V vs Li/Li^+ on amorphous carbon black electrodes) are attractive features that make the molten nitrate and nitrite class of electrolytes interesting for Li/O_2 batteries. Furthermore, we hypothesize that LiO_2 and Li_2O_2 discharge products will have enhanced solubility in this electrolyte compared to room temperature organic electrolytes. Together with improved electrode kinetics at elevated temperature, we anticipate high reversibility and higher rate capability for the oxygen electrode.

In this work, we report that eutectic molten nitrate salt mixtures, such as $LiNO_3$–KNO_3 (melting point: ∼125 °C) and $LiNO_3$–KNO_2–$CsNO_3$ (melting point: ∼90 °C) are currently the most stable Li^+-bearing electrolytes known for the reversible oxygen electrochemistry occurring at the Li/O_2 battery cathode. We confirm our results by combining quantitative gas analysis using pressure monitoring and mass spectrometry with precise coulometry to analyze O_2 electrode processes, along with powder X-ray diffraction (PXRD), scanning electron microscopy (SEM) and elemental analysis to characterize the O_2 electrode products. Our results represent a significant step forward in understanding the necessary requirements for appropriate electrolyte design in a Li/O_2 battery.

2. EXPERIMENTAL DETAILS

$LiNO_3$, KNO_3, KNO_2, and $CsNO_3$ were purchased from Sigma-Aldrich, vacuum-dried at 120 °C for 1 week and stored inside an Ar-filled glovebox. Table 1 summarizes molar ratio and chemical composition of each of the tested electrolytes. Typically, a 12 mm diameter glass microfiber separator (Whatman) was impregnated with 300 mg (∼150 μL) of eutectic mixture and then vacuum-dried at 200 °C (above the eutectic melting point) for 1 day using an oven (LC Technology Solutions) inside the glovebox. For trace amounts of water in the electrolyte, Karl Fischer titration was performed using dry *N*-methylacetamide solvent (NMA, 5 ppm of H_2O, Sigma-Aldrich) before and after the addition of the 300 mg of dried binary or ternary mixture of nitrate/nitrite salts. Results show that water content of 10 ppm is typically observed with these electrolytes. The O_2 electrode consisted of Super P carbon black (Timcal) mixed with PTFE binder (Sigma-Aldrich) in a 95:5 mass ratio (no catalyst). The amorphous carbon was used as received with no pretreatment or surface activation. Super P carbon and PTFE were mixed together in a water-isopropanol mixture and dried in air at room temperature. The mixture was then dry pressed on a 10 mm diameter stainless steel mesh. Typical carbon loading in these batteries was 3–5 mg/cm^2 and electrode surface area was 0.785 cm^2. To improve electrolyte infusion into the porous carbon O_2 cathode, electrolyte separators containing the molten salts and carbon cathode were dried together at 180 °C for 1 day under a vacuum. Carbon oxidation in the presence of molten nitrate was assessed by TGA-mass spectrometry and no carbon dioxide was detected while maintaining Super P carbon and $LiNO_3$–KNO_3 melt under O_2 at 200 °C for 1 week.

Table 1. Molten Salt Electrolytes Used in This Work[a]

electrolyte	chemical composition (mol %)	melting point (°C)	Li^+ transference number	ionic conductivity (mS/cm, 150 °C)
$LiNO_3$–KNO_3	42–58	125	0.68	88
$LiNO_3$–KNO_2–$CsNO_3$	37–39–24	90	0.28	115

[a]Chemical composition, melting point measured by DSC, Li^+ transference number determined by the Bruce and Vincent method, and ionic conductivity at 150 °C.

Typical Li/O_2 lab-type batteries consist of hermetically sealed stainless steel fixtures (Swagelok) of known volume, which is comprised of a pressure sensor (Omega) and a valve (Valco Instruments) that can easily be connected to a mass spectrometer for qualitative and quantitative gas analysis. Together with pressure monitoring, precise concentrations of consumed and evolved oxygen gas during cycling can be determined. Batteries are routinely leak-tested with helium gas at 150 °C prior to use. The anode consists of an 8 mm diameter lithium metal disc (250 μm thick) used as received (MTI Corporation). Once electrolyte and cathode were added into the battery, a stainless steel spring was used to accommodate volume changes upon electrolyte melting and to maintain good electrical contact. All battery construction was performed in an Ar-filled glovebox with O_2 and H_2O levels maintained below 0.1 ppm. Batteries were purged with pure oxygen (Research 5.0 grade, Airgas) at room temperature and maintained under positive pressure, typically around $1.1e^5$–$1.5e^5$ Pa (1.1–1.5 bar). Batteries were then transferred to an oven kept at either 120 or 150 °C depending on the molten nitrate/nitrite salts used. Open-circuit voltage, with periods of typically 6 or 12 h, was applied to ensure both the battery voltage and the pressure reached equilibrium. In this work, current density is reported in mA/gram of carbon contained in the positive electrode. Capacities are reported in mAh/gram of carbon (the areal capacity in mAh/cm^2 can be obtained from carbon loading).

Cyclic voltammetry and galvanostatic cycling at various current densities were used to evaluate battery performance (capacity, voltage)

DOI: 10.1021/jacs.5b11744
J. Am. Chem. Soc. 2016, 138, 2656–2663

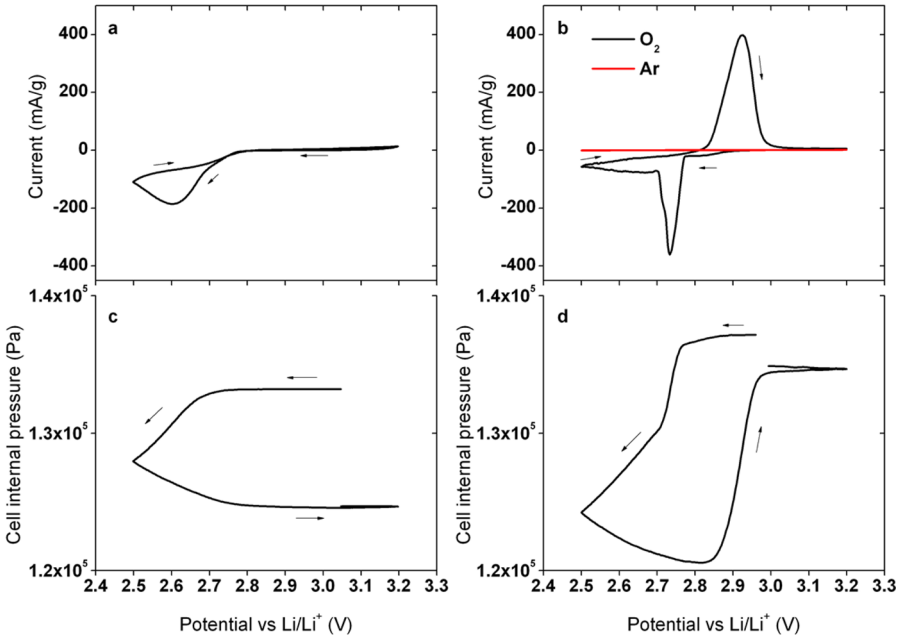

Figure 1. Cyclic voltammetry of O_2 reduction in a Li/O_2 battery electrolyte: (a,c) 0.1 M $LiClO_4$–DMSO at 30 °C and (b,d) $LiNO_3$–KNO_3 eutectic at 150 °C. Working electrode: Super P porous carbon (A = 0.785 cm^2), carbon loading ∼5 mg/cm^2. Counter and reference electrodes: Li metal. Scan rate: 0.05 mV/s. Voltage window: 2.5–3.2 V vs Li/Li^+. Current density expressed in mA per g of carbon.

and O_2 electrode reversibility. For experiments performed in organic electrolytes, battery grade premixed solution of lithium perchlorate ($LiClO_4$, 0.1 mol/L) and dimethyl sulfoxide (DMSO) was purchased from BASF (<10 ppm water measured by Karl Fischer titration). A 12 mm diameter Whatman separator impregnated with 150 μL of electrolyte was used in the battery. Li_2O_2 solubility and diffusivity in the molten nitrate electrolyte was investigated by rotating disk electrode (RDE) measurements. Typically a PTFE-based electrochemical cell was used inside an Ar-filled glovebox. The working electrode consisted of a Pt RDE (5.0 mm OD, 99.99% pure, mirror polished, Pine Research), the counter electrode a Pt wire (1.0 mm OD, Sigma-Aldrich) and the reference electrode a Li metal rod (Sigma-Aldrich). For product characterization, PXRD (Philips X'PERT XRD system with Cu Kα1 radiation, λ = 1.5406 Å) was performed on carbon electrodes at different stages of cycling. Typically the air cathode was extracted from heated batteries inside an Ar-filled glovebox and rinsed with NMA solvent to remove residual nitrate/nitrite salts. The carbon electrode was then sealed in Kapton tape for protection against air contamination. SEM analysis was performed in a Versa 3D DualBeam focused ion beam (FIB) microscope (FEI), and the elemental analysis with a ZEISS 1550VP FESEM microscope equipped with an Oxford X-Max SDD X-ray energy dispersive spectrometer. Similar to PXRD, the carbon cathodes were rinsed with NMA prior to transferring them inside the instrument. For gas analysis, mass spectrometry was performed both during cycling (typically during the battery charge cycle, under "vacuum" conditions) or ex situ using a calibrated Stanford Research Systems RGA100 residual gas analyzer (1–100 AMU range) attached to a high vacuum system (<1.33e^{-6} Pa, Pfeiffer Vacuum). Ex situ measurements were performed at controlled pressure and temperature.

3. RESULTS AND DISCUSSION

Figure 1 compares cyclic voltammograms of O_2 reduction at a Super P carbon cathode in a) conventional Li/O_2 battery electrolyte 0.1 M $LiClO_4$–DMSO and b) $LiNO_3$–KNO_3 eutectic, at 30 and 150 °C, respectively. As expected, results indicate that in the common organic electrolyte, O_2 reduction to form lithium peroxide is a highly irreversible electrochemical process, as only a strong cathodic current and no anodic current is observed in the operating potential window. Previous results have shown that high anodic potentials (>3.8 V) are necessary to oxidize Li_2O_2 in DMSO-based electrolytes, although at these potentials, a substantial fraction of the Li_2O_2 oxidation current results in parasitic decomposition of the electrolyte. On the other hand, CV performed in the O_2-saturated $LiNO_3$–KNO_3 eutectic at 150 °C shows high reversibility with Q_a/Q_c ratio of ∼0.9 (anodic charge Q_a and cathodic charge Q_c were obtained by integrating the "current vs time" plot derived from the CV; Q_a/Q_c would ideally equal 1). To verify nitrate electrolyte electrochemical stability in the operating voltage window, we performed the same CV experiment under Ar gas (without any O_2 present) and did not observe any faradaic currents. Furthermore, pressure monitoring clearly demonstrates gas is consumed upon reduction (cathodic scan) and generated upon oxidation (reverse, anodic scan). Mass spectrometry on the headspace following the CV indicates that only O_2, and no other gas, is evolved during the anodic scan. As expected, no pressure rise is observed during the anodic CV scan of a DMSO-based battery (Figure 1c), as no anodic current is observed, indicating no product is being oxidized. The standard electrode potential (E^0) for the electrochemical formation of Li_2O_2 ($2Li^+ + O_2 + 2e^- \leftrightarrows Li_2O_2$) can be calculated from the free energy of formation, and is generally considered to be ∼2.96 V vs Li/Li^+ at 30 °C. However, operating the battery as 150 °C gives a calculated potential of ∼2.83 V vs Li/Li^+, which agrees with the median potential, measured from the cyclic voltammogram (Figure 1b).

Of importance, quasi-reversible CVs are observed at a carbon O_2 electrode in the molten salt eutectic, with cathodic peak-to-anodic peak separation of about 200 mV. Typical CVs for conventional organic electrolytes at room temperature usually display anodic peaks in the 3.4–4.5 V window, which are attributed to side reactions (e.g., solvent decomposition) alongside direct Li_2O_2 oxidation. Greater currents are obtained when using the molten salt electrolyte, which likely is a result of

DOI: 10.1021/jacs.5b11744
J. Am. Chem. Soc. 2016, 138, 2656–2663

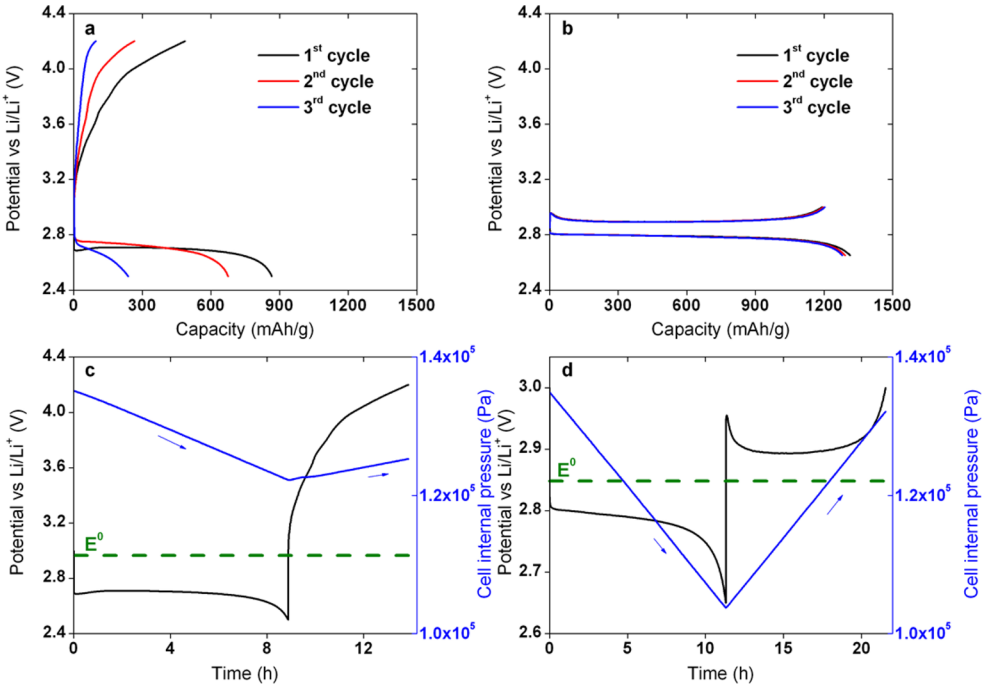

Figure 2. Li/O_2 battery voltage and pressure profiles measured in (a,c) 0.1 M $LiClO_4$–DMSO at 30 °C between 2.5 and 4.2 V and (b,d) $LiNO_3$–KNO_2–$CsNO_3$ molten salt electrolyte at 120 °C between 2.65 and 3.0 V. Positive electrode: Super P carbon:PTFE 95:5 wt %, current: 0.25 mA (~80 mA/g carbon). Electrolyte loading: 150 μL. Carbon loading: ~4 mg/cm^2. Pressure profiles depicted in (c) and (d) are for the first cycle of the battery. Battery capacity expressed in mAh per g of carbon. E^0 represents the thermodynamic potential for the reaction $2Li^+ + 2e^- + O_2 \leftrightarrows Li_2O_2$ at 30 °C (c) and 120 °C (d).

less cathode passivation due to the higher solubility of intermediate LiO_2 and discharge product Li_2O_2. The high cathodic peak potential for O_2 reduction in the melt (~2.73 V vs Li/Li^+) is likely a result of a combination of the following effects: (1) improved electrode kinetics from elevated temperature operation, (2) lower internal cell resistance as a result of high ionic conductivity of the molten salt, (3) improved intermediate solubility (as will be conclusively shown later), such as lithium superoxide (LiO_2), which in turn reduces Li_2O_2-induced electrode passivation.[18,19] Consistent with a Q_a/Q_c ratio of ~0.9, a slight inefficiency in the pressure profile (Figure 1d) is attributed to lithium peroxide precipitating in the separator, away from the current collector carbon and becoming electrically disconnected. Some dissolved lithium peroxide may also have traveled across the electrolyte and was reduced to Li_2O on Li metal. No particular effort was made to optimize the porous volume and electrode architecture to date. These results constitute a significant step forward in the search for stable electrolyte materials. We anticipate that the LiO_2 or Li_2O_2 could react with carbon at the operating temperature of our batteries to generate lithium carbonate (Li_2CO_3) at the surface of carbon. This is consistent with O_2 consumption/evolution inefficiencies observed during the CV.

TGA-MS analysis of a Super P carbon-PTFE:Li_2O_2:$LiNO_3$–KNO_3 1:1:3 mass ratio sample intimately mixed inside an Ar-filled glovebox and held at 200 °C under either Ar or O_2 for 60 h each did not show any mass loss or CO_2 evolution (Figure S1). This suggests that Li_2O_2 would be more stable toward carbon, and Li_2CO_3 would result from a reaction between carbon and reactive intermediate LiO_2. TGA-MS analysis was also performed on a $LiNO_3$–KNO_3:Li_2O_2 mixture (85:15 wt %) to evaluate chemical stability of lithium peroxide in the molten salt (Figure S2). Typically, the sample was heated up to 150 °C, held at this temperature for 5 h, and finally heated up to 500 °C. All heating rates were 2 °C/min. Expected thermal decomposition of lithium peroxide ($2Li_2O_2 \rightarrow 2Li_2O + O_2$, ~35% mass loss starting at about 250 °C) was observed together with O_2 evolution, therefore suggesting Li_2O_2 is chemically stable in the melt below 250 °C.

Figure 2 shows cycling data recorded at 0.25 mA constant current (~0.32 mA/cm^2 or ~80 mA/g) with battery O_2 partial pressure monitoring depicted in Figure 2c,d, where the first cycle pressure profile is shown. As in the CV experiment, both batteries used the same carbon porous electrode with comparable carbon loading, the only difference being the temperature of operation and the electrolyte employed. The battery depicted in Figure 2a and 2c operates in 0.1 M $LiClO_4$–DMSO electrolyte at 30 °C, whereas the battery depicted in Figure 2b and 2d uses a $LiNO_3$–KNO_2–$CsNO_3$ eutectic mixture and cycles at 120 °C. The ternary mixture of nitrate/nitrite salts has a lower melting point compared to the lithium/potassium nitrate binary mixture and therefore allowed us to operate the battery at a lower temperature. Table 1 summarizes chemical composition, melting point measured by differential scanning calorimetry (DSC), lithium cation transference number determined by the Bruce and Vincent method, and ionic conductivity measured at 150 °C using a conductivity cell of known cell constant suitable for elevated temperature measurements. The battery that uses the organic electrolyte has poor capacity retention and high voltage hysteresis, whereas the battery using the molten nitrate/nitrite salts can be cycled between 2.65 and 3.0 V with remarkably low voltage hysteresis (~0.1 V) and good capacity retention. Consistent with the CV data, a ~10% irreversible capacity loss is observed in the molten nitrate/nitrite battery. The voltage profile comparison for the first three cycles of the batteries clearly demonstrates the

DOI: 10.1021/jacs.5b11744
J. Am. Chem. Soc. 2016, 138, 2656–2663

superior behavior of the molten salt Li/O_2 battery compared to prior state of the art in terms of (i) dramatically reduced voltage gap, (ii) excellent capacity retention, (iii) clear end of half cycle based on voltage turn-down on discharge and turn-up on charge. The challenge will be to couple the molten nitrate electrolytes with stable cathode materials to achieve long cycle life. Pressure monitoring in the organic electrolyte battery during cycling clearly shows that only a small fraction of O_2 consumed during discharge is evolved during charge. Side reactions govern the electrochemistry and account for rapid capacity fade in the DMSO-based battery. Many authors have reported high chemical instability of DMSO solvent in the Li/O_2 battery.[20,21]

Figure 2d demonstrates that oxygen can be consumed and subsequently evolved with relatively high efficiency ($\Delta P_{charge}/\Delta P_{discharge} \approx 90\%$) when recharging the molten salt battery, with identical slopes of pressure variation within the battery during discharge and charge. Enhanced LiO_2/Li_2O_2 solubility in the melt leads to electrical disconnection and carbon decomposition, and are thought to be responsible for the ~10% irreversible pressure loss during cycling. We found the stoichiometry for the battery reaction, often reported as e^-/O_2 molar ratio in the literature, to be 2.0 by combining coulometry and gas analysis, for both discharge (ORR) and charge (OER) half-cycles. Oxygen partial pressure, internal battery volume and operating temperature are all carefully controlled parameters. Molar ratios that deviate from 2.0 are indicative of parasitic processes occurring during cycling, often related to a reaction between the electrolyte (or the electrode) and reduced forms of oxygen. Gas analysis of the battery headspace is routinely performed to ensure O_2 (mass 32) is the only gaseous species formed during cycling. Typically, gases such as CO (28), CO_2 (44), NO (30) and NO_2 (46) are monitored by mass spectrometry. These would arise from oxidation reactions of the carbon electrode material and the electrolyte materials, namely NO_2^- and NO_3^-.

Figure 3a shows in situ gas analysis performed during a Li/O_2 battery charge half-cycle in $LiNO_3$–KNO_3 electrolyte at 150

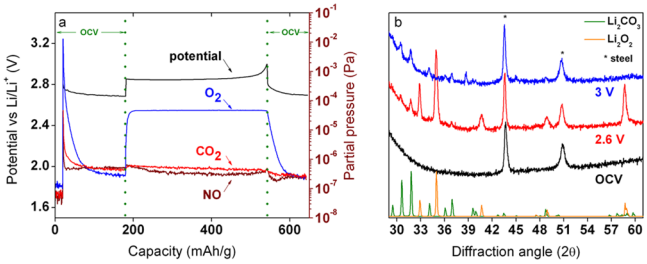

Figure 3. (a) Li/O_2 battery charging profile with in situ gas analysis. Battery employed a $LiNO_3$–KNO_3 molten salt electrolyte, a Super P carbon:PTFE cathode, and was charged at 150 °C, ~80 mA/g, to a 3.0 V cutoff. Capacity expressed in mAh per g of carbon. (b) XRD analysis of a Super P carbon cathode following an OCV period (before discharge), a single discharge to 2.6 V, and a discharge/charge cycle between 2.6 and 3.0 V, in $LiNO_3$–KNO_3 molten salt electrolyte at 150 °C.

°C. The battery was first discharged under O_2 to roughly 30% depth of discharge (~400 mAh/g). Then, during OCV between discharge and charge, the valve connecting the battery to the mass spectrometer was opened and the gases were allowed to flow from the battery headspace directly into the mass spectrometer chamber. The charge half-cycle was therefore carried out under a vacuum which would not be possible with common organic electrolytes due to solvent volatility. As the electrode begins to recharge, oxygen mass 32 signal increases and remains steady throughout the entire charge, which is consistent with the pressure data observed in Figure 2d. Other gases, such as carbon dioxide (mass 44) and nitric oxide (mass 30) remain at background levels. XRD patterns of the carbon electrode before discharge, following a ~1400 mAh/g discharge under O_2 to 2.6 V cathodic cutoff, and after a completed cycle (electrode fully recharged to 3.0 V) are depicted in Figure 3b. The XRD results clearly demonstrate that crystalline Li_2O_2 forms on the carbon surface during discharge and can subsequently be oxidized upon battery charge. XRD also reveals the presence of Li_2CO_3 alongside Li_2O_2, confirming sustained reaction between carbon and the oxygen reduction products.

Lithium peroxide solubility in molten nitrates was investigated by Rotating Disk Electrode (RDE) measurements. The 3-electrode cell was loaded with roughly 35 mL of carefully dried $LiNO_3$–KNO_3 eutectic and maintained at 150 °C by means of thermocouple and suitable beaker heating mantle. Once reproducible cyclic voltammograms were obtained in the 2.8–3.3 V range, Li_2O_2 powder (Alfa Aesar, 95% pure) was added to the molten salt electrolyte, and using the RDE tip, the solution was vigorously stirred for several minutes until saturation. Linear sweep voltammograms (anodic scans from OCV to 3.3 V vs Li/Li^+) were then performed at 1 mV/s, varying the electrode rotation rate from 100 to 2500 rpm. Levich/Cottrell analysis was used to determine bulk concentration and diffusivity of Li_2O_2 in the molten nitrate electrolyte. The Levich equation contains the diffusivity as well as the bulk concentration of the reacting species Li_2O_2, hence one of these quantities must be known to estimate the other (Supporting Information). For that we used the Cottrell equation derived from transient current measurements under quiescent conditions. We measured the peroxide anion concentration to be $5.2e^{-4}$ mol/L, which is an order of magnitude greater than values calculated in organic solvents such as DMSO or DMF at 30 °C (in the 10^{-5} M range). For those organic solvents, lithium atomic absorption spectroscopy (AAS) was typically performed on Li_2O_2-saturated samples after dilution in water.[22] It appears that elevated temperature has an influence on Li_2O_2 solubility, solvation effects between the molten salt electrolyte and the peroxide anions require further investigation. Figure 4a shows linear sweep voltammetry data obtained for Li_2O_2 bulk oxidation at 150 °C at a Pt RDE. Upon addition of lithium peroxide, the open-circuit potential of the battery shifted to ~2.8 V vs Li/Li^+ which is consistent with thermodynamic data. Slightly sloped anodic limiting currents (i.e., mass-transport limited currents) are due to interference with oxidation by impurities in the melt such as NO_2^- and OH^- ions (nitrite ions form when nitrate ions get chemically reduced by the lithium reference electrode, whereas lithium hydroxide is a known impurity in lithium nitrate). Consistent with fast electrode kinetics, the current observed at any given potential along the voltammogram varies linearly with the square root of the rotation rate and the line intercepts the vertical axis at zero (Figure S3).

In the $LiNO_3$–KNO_3 eutectic molten electrolyte, the rate of the electrochemical half-reaction $O_2^{2-} \rightarrow O_2 + 2e^-$ at 150 °C is governed only by mass transport to the electrode surface. A diffusion coefficient of $3.1e^{-8}$ cm^2/s was found for the O_2^{2-} anion, several orders of magnitude lower than typical values for

DOI: 10.1021/jacs.5b11744
J. Am. Chem. Soc. 2016, 138, 2656–2663

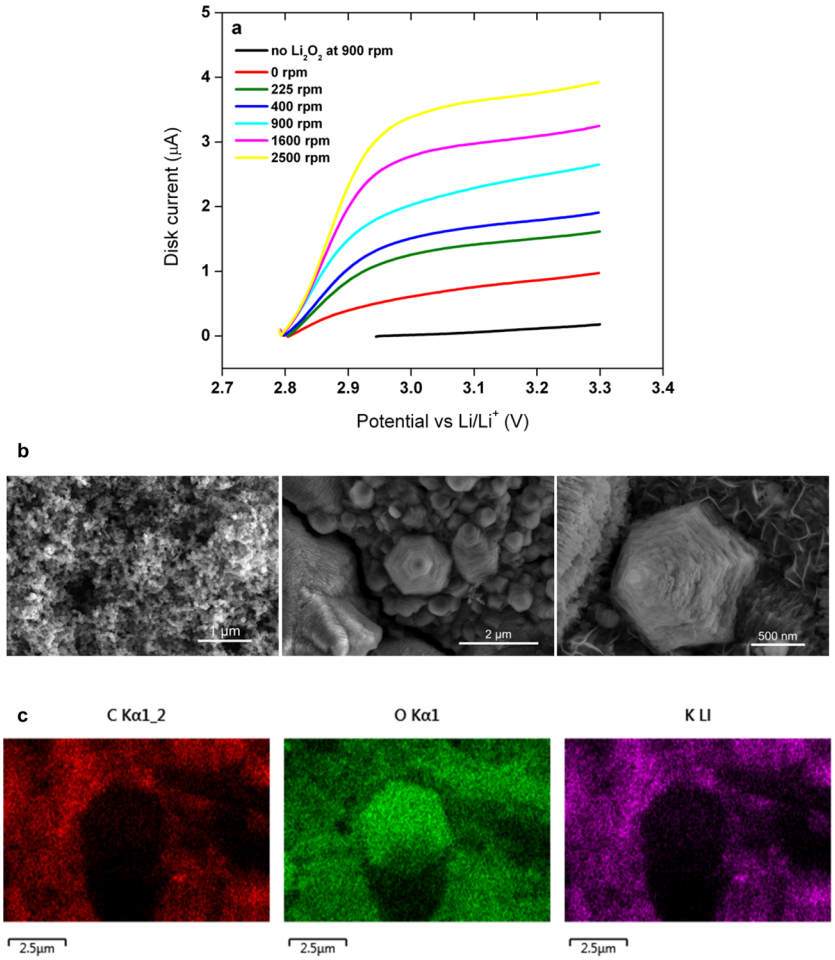

Figure 4. (a) Linear sweep voltammograms recorded at a Pt RDE (A = 0.196 cm^2) from a molten salt electrolyte containing lithium peroxide. v = 1 mV/s, from OCV to 3.3 V vs Li/Li^+. RDE rotation rate increased from 0 to 2500 rpm. For comparison, a LSV scan of the molten salt electrolyte without lithium peroxide was performed at each rotation rate to measure the background current (plotted is the 900 rpm scan). Electrolyte: $LiNO_3$–KNO_3 eutectic. Temperature: 150 °C. Counter electrode: Pt wire, reference electrode: Li metal rod. (b) SEM images of the Super P carbon O_2 electrode. From left to right: electrode before discharge (Super P carbon nanoparticles) and electrode following a ∼1400 mAh/g discharge under O_2 to 2.6 V cathodic cutoff (Li_2O_2 particles). (c) Elemental mapping of carbon, oxygen and potassium centered on a Li_2O_2 crystal, taken from a discharged electrode sample.

O_2 (10^{-5}, 10^{-6} cm^2/s range), but consistent with the fact that peroxide has two negative charges and could exist as an ion pair with Li^+ cations. Appropriate methodology to determine the solubility and diffusivity of oxygen in molten nitrates is being developed.

Further evidence for enhanced solubility of the discharge products was obtained by scanning electron microscopy (SEM) and a morphological study of the discharge products in the O_2 electrode. Typically, large particles ranging from 500 nm to several microns were observed at the carbon surface. The observed morphology of Li_2O_2 consists of stacks of hexagonal layers (Figure 4b). This shape corroborates theoretical predictions of the equilibrium Wulff construction of Li_2O_2 as a hexagonal prism.[23,24] We conjecture that a solution-mediated precipitation of lithium peroxide is responsible for the growth of such large crystals. Figure 4b compares SEM images of carbon surface before and after a discharge under O_2 to 2.6 V at 80 mA/g in $LiNO_3$–KNO_3 molten salt. Cathode samples were collected from Li/O_2 batteries and rinsed with NMA solvent to remove residual nitrate salts. Figure 4c displays the elemental analysis performed on a discharged carbon cathode and centered on a grown lithium peroxide crystal.

The data shown in Figures 3 and 4 support the reversible formation of Li_2O_2 in the melt with fast electrode kinetics resulting in extremely low discharge/charge overpotentials (∼50 mV). SEM analysis of a Super P carbon electrode fully charged to 3.0 V (1st cycle) showed no evidence of lithium peroxide, and many areas of the cathode were covered by needle-like particles of several hundred nanometers (Figure S4a). Consistent with XRD data showing Li_2CO_3 at the end of charge, elemental analysis supports the coprecipitation of Li_2CO_3 at the surface (Figure S4b).

The Li/O_2 battery depicted in Figure 5a was galvanostatically cycled in $LiNO_3$–KNO_3 eutectic at 150 °C at 0.5 mA (∼0.64 mA/cm^2 or ∼160 mA/g of carbon) with limited depth of discharge (2 mAh discharge, ∼45% DOD). The battery was stopped after 50 cycles (∼340 h of cycling) when the discharge capacity had significantly dropped and the cathode was analyzed by XRD and SEM. Despite ending the cycling after a complete charging half-cycle to 3.0 V, XRD analysis revealed the presence of Li_2O_2 at the carbon surface, alongside Li_2CO_3 (Figure 5b). We believe that electrically disconnected Li_2O_2 accumulates away from the electrode during cycling while Li_2CO_3 passivates carbon and is responsible for the continuous

DOI: 10.1021/jacs.5b11744
J. Am. Chem. Soc. 2016, 138, 2656–2663

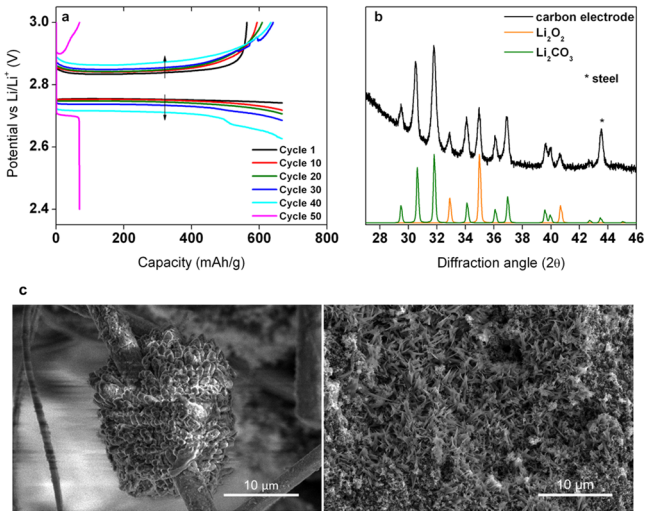

Figure 5. (a) Li/O_2 battery voltage profile for cycle 1, 10, 20, 30, 40, and 50. Battery cycled in $LiNO_3$–KNO_3 molten salt electrolyte at 150 °C using a Super P carbon cathode, current density: ~0.64 mA/cm^2 or ~160 mA/g carbon, carbon loading: ~4 mg/cm^2. Arrows indicate increasing voltage hysteresis with cycle number. (b) XRD pattern of the carbon electrode used in (a) following 50 cycles. Reference patterns of Li_2O_2 (#74–0115) and Li_2CO_3 (#22–1141). (c) SEM images of the O_2 electrode following 50 cycles. Left image: Li_2O_2 particles agglomerating on a separator microfiber away from electrode surface. Right image: Li_2CO_3 particles covering carbon surface.

increase in battery polarization with cycle number. To further support this argument, we performed SEM analysis of the cycled carbon cathode. Large, >10 μm, clusters of Li_2O_2 hexagonal prisms were observed on the residual separator glass microfibers leftover on the carbon side (Figure 5c, left image). This is consistent with uncontrolled reprecipitation of dissolved Li_2O_2 during battery cycling. Large crystals of Li_2CO_3 (fuzzy "needle-like" particles) can be seen throughout the carbon surface (Figure 5c, right image).

A sustained reaction between oxygen reduction products and carbon is responsible for the cycle life limitation of the present batteries. Electrode passivation by Li_2CO_3, often reported as "carbon corrosion", is a known phenomenon in Li/O_2 batteries.[25,26] As the number of cycles increases, the voltage hysteresis of the battery increases, consistent with the growth in electrode impedance (Figure 5a). The focus of future work is on replacing the amorphous carbon with oxidatively stable cathode materials. The origin of capacity fade in these systems is therefore 2-fold. First, one needs to better control Li_2O_2 dissolution and precipitation during discharge, and second, cathode materials stable to O_2 reduction products need to be developed in order to achieve high Coulombic efficiency and maintain high energy efficiency.

4. CONCLUSIONS

We developed chemically stable electrolytes for the Li/O_2 battery by replacing volatile, unstable and air-intolerant aqueous or organic-based electrolytes with an inorganic molten salt. We used eutectic binary or ternary mixtures of alkali metal nitrate/nitrite salts and studied the oxygen electrochemistry at 120 and 150 °C. Oxygen reduction was found to proceed based on a 2 e^-/O_2 reaction leading to the formation of Li_2O_2. We observed the shape of deposited lithium peroxide to be hexagonal, which agrees with equilibrium surface energy calculations and Wulff construction. XRD confirmed the reversible formation of crystalline Li_2O_2, and in situ gas and pressure analyses demonstrated that oxygen could be efficiently evolved during charge at a very low overpotential. A discharge/charge voltage gap of only ~0.1 V constitutes the lowest value ever reported for a Li/O_2 battery. Improved reversibility and rate capability are thought to originate from enhanced solubility of the discharge products, which alleviate the intrinsic electronic transport limitations of Li_2O_2 deposited on the Li/O_2 battery cathode. More fundamental work needs to be done to understand solvation effects and the role of nitrate/nitrite anions in enhancing solubility of the discharge products. In the present study we used Super P carbon as the O_2 electrode material and showed that it tends to react with oxygen reduction products to form lithium carbonate. We also demonstrated that decomposition of the amorphous carbon electrode causes battery failure, and therefore the identification of suitable noncarbonaceous O_2 electrode materials will be key to success for this chemistry. Although we found that Li_2CO_3 is sparingly soluble in the melt and can be bulk oxidized at about 3.5 V vs Li/Li^+ at a Pt disk electrode, the side product passivates the carbon electrode when operating the battery in the typical voltage regime (2.6–3.0 V) and is responsible for increased polarization and capacity loss. XRD analysis of a cycled carbon cathode revealed substantial accumulation of electronically disconnected Li_2O_2. Large clusters, >10 μm in diameter, of Li_2O_2 crystals deposited on the glass fiber separator were observed by SEM. Solubility of Li_2O_2 allows growth of large particles and clusters via a solution phase mechanism which enables high areal capacity and low overpotential, but creates challenges in achieving high Coulombic efficiency. Uncontrolled diffusion and precipitation of soluble Li_2O_2 is a major cause of capacity loss. Proprietary methods to address this issue are presently under development at Liox. The low O_2 solubility is a challenge for achieving high rate capability, and catalytic materials facilitating chemical absorption of O_2 in the molten salt electrolyte are presently being investigated.

■ ASSOCIATED CONTENT

Ⓢ Supporting Information

The Supporting Information is available free of charge on the ACS Publications website at DOI: 10.1021/jacs.5b11744.

TGA-MS analysis of a Super P carbon:PTFE/Li_2O_2/(Li,K)NO_3 mixture; TGA-MS analysis of a (Li,K)NO_3/Li_2O_2 mixture; Levich plot derived from RDE voltammetry study of Li_2O_2 bulk oxidation in (Li,K)-NO_3molten salt; SEM/EDX analysis of a Super P carbon:PTFE air cathode following the first discharge/charge cycle. (PDF)

■ AUTHOR INFORMATION

Corresponding Authors

*vincent@liox.com

*dan@liox.com

Notes

The authors declare no competing financial interest.

■ ACKNOWLEDGMENTS

This work is financially supported as part of the FY 2014 Vehicle Technologies Program Wide Funding Opportunity Announcement, under Award Number DE-FOA-0000991

DOI: 10.1021/jacs.5b11744
J. Am. Chem. Soc. 2016, 138, 2656–2663

(0991-1872), by the U.S. Department of Energy (DOE) and National Energy Technology Laboratory (NETL) on behalf of the Office of Energy Efficiency and Renewable Energy (EERE).

REFERENCES

(1) Abraham, K. M.; Jiang, Z. *J. Electrochem. Soc.* **1996**, *143*, 1−5.
(2) Peng, Z.; Freunberger, S. A.; Chen, Y.; Bruce, P. G. *Science* **2012**, *337*, 563−566.
(3) Christensen, J.; Albertus, P.; Sanchez-Carrera, R. S.; Lohmann, T.; Kozinsky, B.; Liedtke, R.; Ahmed, J.; Kojic, A. *J. Electrochem. Soc.* **2012**, *159*, R1−R30.
(4) Bruce, P. G.; Freunberger, S. A.; Hardwick, L. J.; Tarascon, J.-M. *Nat. Mater.* **2011**, *11*, 19−29.
(5) Sharon, D.; Hirsberg, D.; Afri, M.; Garsuch, A.; Frimer, A. A.; Aurbach, D. *J. Phys. Chem. C* **2014**, *118*, 15207−15213.
(6) Bryantsev, V. S.; Uddin, J.; Giordani, V.; Walker, W.; Addison, D.; Chase, G. V. *J. Electrochem. Soc.* **2013**, *160*, A160−A171.
(7) McCloskey, B. D.; Bethune, D. S.; Shelby, R. M.; Girishkumar, G.; Luntz, A. C. *J. Phys. Chem. Lett.* **2011**, *2*, 1161−1166.
(8) Black, R.; Oh, S. H.; Lee, J.-H.; Yim, T.; Adams, B.; Nazar, L. F. *J. Am. Chem. Soc.* **2012**, *134*, 2902−2905.
(9) Bryantsev, V. S.; Giordani, V.; Walker, W.; Blanco, M.; Zecevic, S.; Sasaki, K.; Uddin, J.; Addison, D.; Chase, G. V. *J. Phys. Chem. A* **2011**, *115*, 12399−12409.
(10) Mccloskey, B. D.; Valery, A.; Luntz, A. C.; Gowda, S. R.; Wallraff, G. M.; Garcia, J. M.; Mori, T.; Krupp, L. E. *J. Phys. Chem. Lett.* **2013**, *4*, 2989−2993.
(11) Chen, Y.; Freunberger, S. A.; Peng, Z.; Fontaine, O.; Bruce, P. G. *Nat. Chem.* **2013**, *5*, 489−494.
(12) Chase, G. V.; Zecevic, S.; Walker, W.; Uddin, J.; Sasaki, K. A.; Giordani, V.; Bryantsev, V.; Blanco, M.; Addison, D. *Soluble Oxygen Evolving Catalysts for Rechargeable Metal-Air Batteries*. US Patent 2012/0028137, April 23, 2010.
(13) Uddin, J.; Addison, D.; Giordani, V.; Chase, G. V.; Walker, W. *Alkali Metal/Oxygen Batteries Employing Molten Nitrate Electrolytes*. WIPO Patent 2014/153551, March 21, 2013.
(14) Raistrick, I. D.; Poris, J.; Huggins, R. A. *Proc. Symp. Lithium Batter.* **1981**, *81*, 477−483.
(15) Miles, M. H. *J. Electrochem. Soc.* **1980**, *127*, 1761−1766.
(16) Zambonin, P. G. *J. Electroanal. Chem. Interfacial Electrochem.* **1971**, *33*, 243−251.
(17) Zambonin, P. G.; Jordan, J. *J. Am. Chem. Soc.* **1969**, *91*, 2225−2228.
(18) Walker, W.; Giordani, V.; Uddin, J.; Bryantsev, V. S.; Chase, G. V.; Addison, D. *J. Am. Chem. Soc.* **2013**, *135*, 2076−2079.
(19) Burke, C. M.; Pande, V.; Khetan, A.; Viswanathan, V.; McCloskey, B. D. *Proc. Natl. Acad. Sci. U. S. A.* **2015**, *112*, 9293−9298.
(20) Kwabi, D. G.; Batcho, T. P.; Amanchukwu, C. V.; Ortiz-Vitoriano, N.; Hammond, P.; Thompson, C. V.; Shao-Horn, Y. *J. Phys. Chem. Lett.* **2014**, *5*, 2850−2856.
(21) Sharon, D.; Afri, M.; Noked, M.; Garsuch, A.; Frimer, A. A.; Aurbach, D. *J. Phys. Chem. Lett.* **2013**, *4*, 3115−3119.
(22) Lopez, N.; Graham, D. J.; McGuire, R., Jr.; Alliger, G. E.; Shao-Horn, Y.; Cummins, C. C.; Nocera, D. G. *Science* **2012**, *335*, 450−453.
(23) Radin, M. D.; Rodriguez, J. F.; Tian, F.; Siegel, D. J. *J. Am. Chem. Soc.* **2012**, *134*, 1093−1103.
(24) Mo, Y.; Ong, S. P.; Ceder, G. *Phys. Rev. B: Condens. Matter Mater. Phys.* **2011**, *84*, 205446.
(25) McCloskey, B. D.; Speidel, A.; Scheffler, R.; Miller, D. C.; Viswanathan, V.; Hummelshøj, J. S.; Nørskov, J. K.; Luntz, A. C. *J. Phys. Chem. Lett.* **2012**, *3*, 997−1001.
(26) Gallant, B. M.; Mitchell, R. R.; Kwabi, D. G.; Zhou, J.; Zuin, L.; Thompson, C. V.; Shao-Horn, Y. *J. Phys. Chem. C* **2012**, *116*, 20800−20805.

DOI: 10.1021/jacs.5b11744
J. Am. Chem. Soc. 2016, 138, 2656−2663